

Nature of the magnetism of iridium in the double perovskite $\text{Sr}_2\text{CoIrO}_6$

S. Agrestini,^{1,2,*} K. Chen,^{3,4} C.-Y. Kuo,^{1,5} L. Zhao,¹ H.-J. Lin,⁵ C.-T. Chen,⁵ A. Rogalev,⁶ P. Ohresser,³ T.-S. Chan,⁵ S.-C. Weng,⁵ A. C. Komarek,¹ K. Yamaura,^{7,8} M. W. Haverkort,⁹ Z. Hu,¹ and L. H. Tjeng¹

¹Max Planck Institute for Chemical Physics of Solids, Nöthnitzerstr. 40, 01187 Dresden, Germany

²ALBA Synchrotron Light Source, E-08290 Cerdanyola del Vallès, Barcelona, Spain

³Synchrotron SOLEIL, L'Orme des Merisiers, Saint-Aubin, 91192 Gif-sur-Yvette, France

⁴Institute of Physics II, University of Cologne, Zùlpicher Straße 77, 50937 Cologne, Germany

⁵National Synchrotron Radiation Research Center, 101 Hsin-Ann Road, Hsinchu 30076, Taiwan

⁶ESRF-The European Synchrotron, 71 Avenue des Martyrs, 38000 Grenoble, France

⁷Research Center for Functional Materials, National Institute for Materials Science, 1-1 Namiki, Tsukuba, Ibaraki 305-0044, Japan

⁸Graduate School of Chemical Sciences and Engineering, Hokkaido University, North 10 West 8, Kita-ku, Sapporo, Hokkaido 060-0810, Japan

⁹Institute for theoretical physics, Heidelberg University, Philosophenweg 19, 69120 Heidelberg, Germany
(Dated: November 26, 2021)

We report on our investigation on the magnetism of the iridate double perovskite $\text{Sr}_2\text{CoIrO}_6$, a nominally Ir^{5+} Van Vleck $J_{eff} = 0$ system. Using x-ray absorption (XAS) and x-ray magnetic circular dichroism (XMCD) spectroscopy at the Ir- $L_{2,3}$ edges, we found a nearly zero orbital contribution to the magnetic moment and thus an apparent breakdown of the $J_{eff} = 0$ ground state. By carrying out also XAS and XMCD experiments at the Co- $L_{2,3}$ edges and by performing detailed full atomic multiplet calculations to simulate all spectra, we discovered that the compound consists of about 90% Ir^{5+} ($J_{eff} = 0$) and Co^{3+} ($S = 2$) and 10% Ir^{6+} ($S = 3/2$) and Co^{2+} ($S = 3/2$). The magnetic signal of this minority Ir^{6+} component is almost equally strong as that of the main Ir^{5+} component. We infer that there is a competition between the Ir^{5+} - Co^{3+} and the Ir^{6+} - Co^{2+} configurations in this stoichiometric compound.

PACS numbers: 71.70.Ch, 75.70.Tj, 78.70.Dm, 72.80.Ga

I. INTRODUCTION

Recently, correlated oxides with strong spin-orbit coupling (SOC) have attracted a tremendous interest because the associated entanglement of the spin and orbital degrees of freedom may give rise to unexpected exotic electronic states. In the case of iridates with Ir^{4+} ($5d^5$) in octahedral coordination the strong SOC can lead to the so-called $J_{eff} = 1/2$ state by splitting the t_{2g} states into a full $j_{eff} = 3/2$ band and a half-filled $j_{eff} = 1/2$ band¹. This spin-orbit entangled $J_{eff} = 1/2$ state renders the Mott insulator behavior observed in many iridium oxides like Sr_2IrO_4 ^{1,2} and has been proposed to provide in honeycomb d^5 systems like $(\text{Li},\text{Na})_2\text{IrO}_3$ ^{3,4} and RuCl_3 ^{5,6} the needed prerequisites for the long-sought materialization of the Kitaev model and the emergence of Majorana fermions⁷.

Applying the same picture of a strong SOC limit to transition metals with d^4 configuration, e.g. Ru^{4+} , Os^{4+} , and Ir^{5+} , the $j_{eff} = 3/2$ quadruplet is filled with four electrons and the $j_{eff} = 1/2$ doublet is completely empty, which leads to a Van Vleck singlet ground state $J_{eff} = 0$. In contrast to these expectations, some Ru^{4+} oxides like Ca_2RuO_4 are known to show an antiferromagnetic ground state^{8,9}. Recently, theoretical studies have suggested that strong inter-site hopping may lead to superexchange interactions large enough to cause an exciton condensation, or more accurately, a condensation of $J_{eff} = 1$ triplon excitations, and to drive the

antiferromagnetism or ferromagnetism in such nominally Van Vleck d^4 systems¹⁰⁻¹². Later works however, suggested that the interatomic exchange in Ir^{5+} double perovskites might be too weak to overcome the singlet-triplet gap^{13,14}. Experimentally, on the one hand, Cao et al.¹⁵ reported an antiferromagnetic long-range order in the double perovskite Sr_2YIrO_6 and, to explain the magnetic order, argued that the non-cubic crystal field would cause a suppression of the excitation gap and, as a result, the breakdown of the $J_{eff} = 0$ state. On the other hand, a study combining XMCD measurements and full atomic multiplet cluster calculations demonstrated the stability of the Van Vleck singlet state of Ir^{5+} , even in presence of strong tetragonal crystal distortions like in $\text{Sr}_2\text{Co}_{0.5}\text{Ir}_{0.5}\text{O}_4$ ¹⁶. A very recent resonant inelastic x-ray scattering study determined the dispersion of the triplet and quintet states in the double perovskites $(\text{Ba},\text{Sr})_2\text{YIrO}_6$ to be less than 50 meV, i.e. much smaller than the excitation gap, ruling out the possibility of a $J_{eff} = 1$ excitonic condensation¹⁷. The origin of the magnetism reported in the double perovskite Sr_2YIrO_6 and Ba_2YIrO_6 is also debated in a number of other papers¹⁸⁻²¹.

In this context, the magnetism of the Ir^{5+} ion in the double perovskite $\text{Sr}_2\text{CoIrO}_6$ is a very interesting case. In this compound the large difference in cation radii causes the cobalt ions to form a three dimensional alternate arrangement with the iridium ions. Neutron diffraction and susceptibility measurements detected the onset of a long range antiferromagnetic order of the cobalt

moments at $T_N \sim 130$ K^{22,23}. The Iridium ions, instead, were considered to be paramagnetic. Bond valence sums and band structure calculations predicted $\text{Sr}_2\text{CoIrO}_6$ to have a high spin (HS, $S = 2$) Co^{3+} and low spin (LS) Ir^{5+} state²². Surprisingly, a subsequent XMCD study of the $\text{La}_{2-x}\text{Sr}_x\text{CoIrO}_6$ system reported that the Ir^{5+} has a paramagnetic moment with almost no orbital contribution²⁴, implying that the $J_{eff} = 0$ state does not form the ground state. This finding is in contradiction with XMCD studies on other iridates where the Ir^{5+} XMCD signal does indicate the presence of an orbital moment^{16,25}.

Here we address the $\text{Sr}_2\text{CoIrO}_6$ issue by carrying out XAS and XMCD measurements not only on the Ir- $L_{2,3}$ edges but also on the Co- $L_{2,3}$ together with detailed calculations to explain the spectra. Our first objective is to verify whether the valence state of the Ir and Co is 5+ and 3+, respectively, and whether the system is stoichiometric. We then aim to determine what the magnetic ground state is of the Ir^{5+} ions producing possibly such an unusual spectral shape that may indicate the absence of orbital contribution to the paramagnetic moment.

II. EXPERIMENTAL

The $\text{Sr}_2\text{CoIrO}_6$ sample was grown from appropriate amounts of SrCO_3 , Co_3O_4 and IrO_2 that were mixed and ground together. The mixture was pressed into a pellet that was sintered for 22 h at 1180 °C in air, followed by a final sintering for more than two days in a flow of oxygen (\sim ambient pressure).

The XAS at the Co- $L_{2,3}$ edge was recorded in the total electron yield mode at the Dragon beamline of the NSRRC in Taiwan with a photon-energy resolution of 0.25 eV. A single crystal of CoO was measured simultaneously in a separate chamber to obtain relative energy referencing with better than a few meV accuracy at the Co- L_3 edge (780 eV). The sample pellets were fractured in situ in order to obtain a clean surface. The pressure was below 1×10^{-9} mbar during the measurements. The XAS at the Co- K and Ir- L_3 edges were measured in fluorescence yield and transmission modes at the 16A1 and 07A1 beamlines of the NSRRC, respectively. The XMCD spectra at the Co- $L_{2,3}$ edges of $\text{Sr}_2\text{CoIrO}_6$ were collected at the DEIMOS beamline²⁶ of the synchrotron SOLEIL in Paris (France) with a photon-energy resolution of 0.2 eV and a degree of circular polarization close to 100%. The sample was measured at $T = 50$ K and in a magnetic field of 6 T. The spectra were recorded using the total electron yield method. The sample was also fractured in situ in order to obtain a clean surface. The XMCD measurements at the Ir- $L_{2,3}$ edges were performed at the ID12 beamline²⁷ of the European Synchrotron Radiation Facility (ESRF) using the fluorescence yield detection mode. The degree of circular polarization was about 97%. A self-absorption correction was applied to the Ir- $L_{2,3}$ XAS measured with right

and left circular polarized light. Finally the Ir- L_3/L_2 edge-jump intensity ratio $I(L_3)/I(L_2)$ was normalized to 2.22²⁸. This takes into account the difference in the radial matrix elements of the $2p_{1/2}$ -to- $5d(L_2)$ and $2p_{3/2}$ -to- $5d(L_3)$ transitions. The XMCD spectra were obtained as the direct difference between consecutive x-ray absorption near edge spectroscopy (XANES) scans recorded with opposite helicities of the incoming x-ray beam in 17 T at low temperature of 2 K.

III. THEORETICAL CALCULATIONS

The configuration-interaction cluster calculations were performed using the Quany Package²⁹⁻³¹. The method uses an IrO_6 and CoO_6 cluster, which includes explicitly the full atomic multiplet interaction, the hybridization of Ir and Co with the ligands, the crystal field acting on the Ir and Co ions, and the crystal field acting on the ligands. The hybridization strengths and the crystal field parameters were extracted ab initio by DFT calculations carried out using the full-potential local-orbital code FPLO³². The non-cubic crystal field acting on the Ir and Co ions was varied to best fit the experimental XAS and XMCD spectra. The parameters used in the calculations for the Co and Ir ions are listed in Ref.³³ and³⁴, respectively. Since we are dealing with a polycrystalline sample, we simulated the experimental data by summing two calculated spectra: one for circularly polarized light with the Poynting vector in the xy plane and one with the Poynting vector along the z axis, with a weighting ratio of 2:1. For all simulations we have considered the thermal population of the different states using a Boltzmann distribution.

IV. EXPERIMENTAL RESULTS

A. Co- K and Ir- L_3 XAS

To check the Co valence we have measured the Co- K edge XAS taken with TFY for $\text{La}_2\text{CoIrO}_6$, $\text{Ca}_3\text{CoRhO}_6$, $\text{Sr}_2\text{CoIrO}_6$ and EuCoO_3 , as shown in Fig. 1a. Although the spectral features of the Co- K edge are strongly affected by the local crystal structure, the valence state of Co can still be determined³⁵ by the energy position of the steepest slope of the absorption edge. Here we can see that the energy position in $\text{Sr}_2\text{CoIrO}_6$ is the same as that of the Co^{3+} reference sample LaCoO_3 , and is about 1.7 eV higher than that of $\text{La}_2\text{CoIrO}_6$ with a Co^{2+} state, which suggests a mainly 3+ valence of the cobalt ions in $\text{Sr}_2\text{CoIrO}_6$. Similar results were obtained previously by A. Kolchinskaya et al.²⁴.

Having determined a mainly Co^{3+} state in $\text{Sr}_2\text{CoIrO}_6$, we turn to the Ir- L_3 XAS spectra to probe the valence of the iridium ions. Fig. 1b reports the Ir- L_3 XAS spectrum of $\text{Sr}_2\text{CoIrO}_6$ together with the spectra of IrCl_3 ,

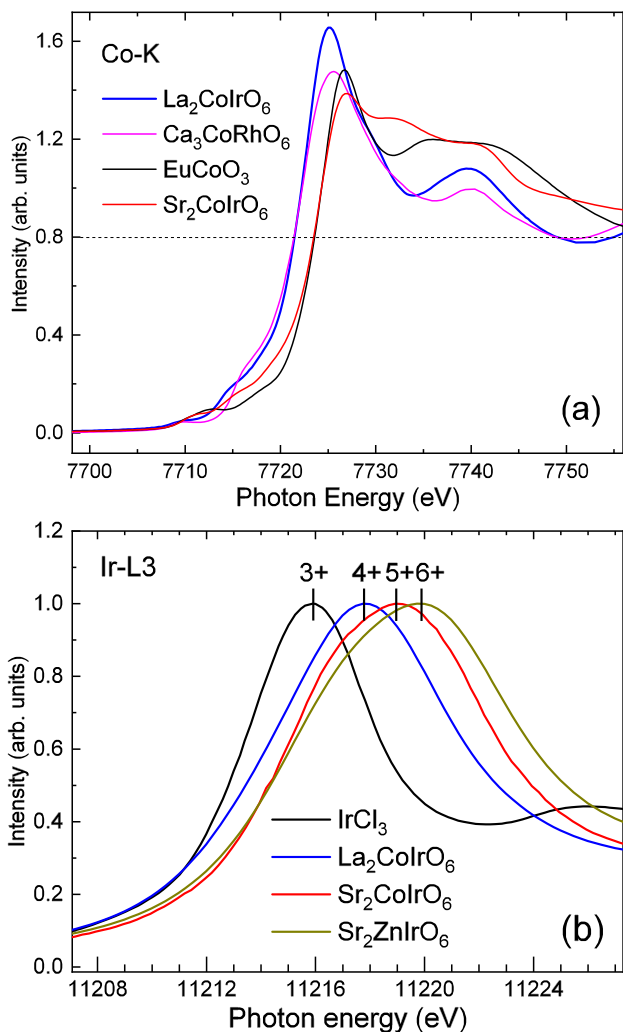


FIG. 1: (a) The Co- K edge XAS spectra of Sr₂CoIrO₆ and of La₂CoIrO₆, and Ca₃CoRhO₆ as Co²⁺ references, and EuCoO₃ as Co³⁺ reference. (b) The Ir- L_3 XAS spectra of Sr₂CoIrO₆ and of IrCl₃ as Ir³⁺ reference, La₂CoIrO₆, and Sr₂ZnIrO₆ as Ir⁶⁺ reference.

La₂CoIrO₆ and Sr₂ZnIrO₆ as Ir³⁺, Ir⁴⁺, and Ir⁶⁺ reference compounds, respectively. It is well known that XAS spectra at the transition metal $L_{2,3}$ edge are highly sensitive to the valence state: an increase of the valence state of the metal ion by one results in a shift of the $L_{2,3}$ XAS spectra by one or more eV toward higher energies, as shown by XAS studies on many oxides^{36–39}, including iridium oxides^{25,40,41}. This shift is due to a final state effect in the x-ray absorption process. The energy difference between a d^n (e.g. d^4 for Ir⁵⁺) and a d^{n-1} (e.g. d^3 for Ir⁶⁺) configuration is approximately $\Delta E = E(2p^6d^{n-1} \rightarrow 2p^5d^n) - E(2p^6d^n \rightarrow 2p^5d^{n+1}) = U_{pd} - U_{dd} \sim 1-2$ eV, where U_{dd} is the Coulomb repulsion energy between two d electrons and U_{pd} the one between a d electron and the $2p$ core hole.

One can see that the white line of Sr₂CoIrO₆ is shifted by ~ 1.3 eV to higher energies with respect to that of

Ir⁴⁺ in La₂CoIrO₆, but is shifted by ~ 1 eV to lower energies with respect to that of Ir⁶⁺ oxide Sr₂ZnIrO₆. This energy shift thus indicates a reasonable increase of Ir valence state from 4+ to 5+ and further to 6+ going from La₂CoIrO₆ to Sr₂CoIrO₆ and further to Sr₂ZnIrO₆. A similar energy shift of the white line position was previously observed going from Sr₃ZnIr⁴⁺O₆ to Sr₃NaIr⁵⁺O₆ and further to Nd₂K₂Ir⁶⁺O₇⁴². Our experimental results are different from the previous study in ref²⁴, where no energy shift of the Ir- L_3 white-line was observed. Our results are consistent with the above finding of mainly Co³⁺ in Sr₂CoIrO₆ observed from the Co- $L_{2,3}$, fulfilling the charge balance requirement. It should be noted, however, that the Ir- L_3 XAS data reported in Fig. 1b cannot exclude the presence of a minor amount of Ir⁴⁺ or Ir⁶⁺ ions coexisting with the majority of Ir⁵⁺ ions.

B. Co- $L_{2,3}$ XAS

Fig. 2 shows the room temperature Co- $L_{2,3}$ XAS of Sr₂CoIrO₆ (red line) together with the spectra of EuCoO₃ (olive green) as a LS-Co³⁺ reference, Sr₂CoRuO₆ (black line) as a HS-Co³⁺ reference⁴³, La₂CoIrO₆ (blue line) and CoO (green line) as Co²⁺ references. As it can be seen in Fig. 2, the XAS of Sr₂CoIrO₆ has the centers of gravity of the Co- L_2 and L_3 white lines lying at the same energies as those of Sr₂CoRuO₆ and EuCoO₃, and about 1.2 eV higher in energy than those of La₂CoIrO₆ and CoO. Hence, our experimental Co- $L_{2,3}$ XAS data indicate the cobalt valence state in Sr₂CoIrO₆ and La₂CoIrO₆ to be 3+ and 2+, respectively. However, we would like also to point out the presence of a minor prepeak at 778 eV in the spectrum of Sr₂CoIrO₆. A similar prepeak is also present in the spectrum of Sr₂CoRuO₆ and was attributed in literature to the presence of a Co²⁺ species⁴³. By subtracting a 10% Co²⁺ spectrum from the as measured spectrum of Sr₂CoIrO₆ one can obtain a XAS spectrum free from any features in the pre-peak region. A two-component scenario with similar amounts of Co²⁺ species was previously reported in literature in thin films of Sr₂CoIrO₆⁴⁴.

Another unique feature of the $L_{2,3}$ XAS spectra is that the dipole selection rules are very sensitive in determining which of the $2p^53d^{n+1}$ final states can be reached and with what intensity, starting from a particular $2p^63d^n$ initial state ($n = 6$ for Co³⁺ and $n = 7$ for Co²⁺). This makes the technique extremely sensitive to the symmetry of the initial state, i.e., the spin state and local environment of the Co ions^{45–50}. Despite having the same Co³⁺ valence, the line shape of the Co- $L_{2,3}$ edge spectrum of Sr₂CoIrO₆ is very different from that of EuCoO₃ but in very good agreement with that of Sr₂CoRuO₆. This shows that the ground state of the Co ions in Sr₂CoIrO₆ is different from the LS $S = 0$ state of EuCoO₃⁴⁵ and is the same as the HS $S = 2$ state of Sr₂CoRuO₆⁴³. The spin only effective magnetic moment of HS Co³⁺ is $\mu_{eff} = 4.9 \mu_B/\text{f.u.}$ This value in good agreement with

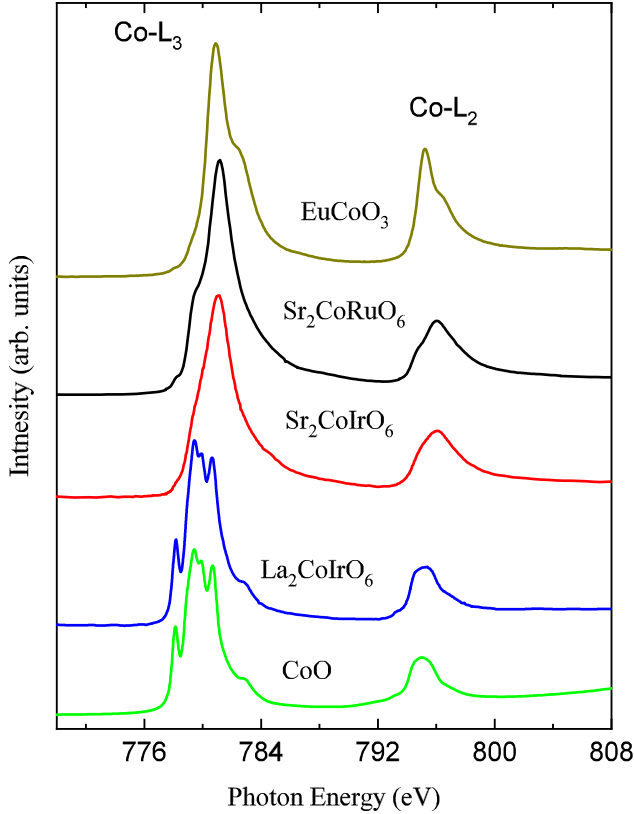


FIG. 2: The Co- $L_{2,3}$ absorption of $\text{Sr}_2\text{CoIrO}_6$ (red lines) together with EuCoO_3 (olive green), as a LS- Co^{3+} reference, $\text{Sr}_2\text{CoRuO}_6$ (black line) as a HS- Co^{3+} reference, $\text{La}_2\text{CoIrO}_6$ (blue line) and CoO (green line) as a Co^{2+} references.

the effective magnetic moment $\mu_{eff} = 5.1 \mu_B/\text{f.u.}$ determined from magnetic susceptibility measurements²² assuming a small magnetic moment of the Van Vleck Ir^{5+} ions.

C. Co- $L_{2,3}$ XMCD

Fig.3 shows the Co- $L_{2,3}$ isotropic XAS and XMCD data (red circles) measured on $\text{Sr}_2\text{CoIrO}_6$ with circular polarized light. The XMCD is defined as the difference between the x-ray absorption spectra taken with the photon spin of the circular polarized light parallel and antiparallel aligned to the magnetic field. In Fig. 3 we have reported also the theoretical Co- $L_{2,3}$ XAS and XMCD spectra for the Co^{3+} in the HS ($S = 2$) configuration (blue lines) as obtained from our full-multiplet configuration-interaction calculations. The HS Co^{3+} simulation can nicely reproduce the line-shape of the measured Co- $L_{2,3}$ XMCD spectrum of $\text{Sr}_2\text{CoIrO}_6$ except for the minor prepeak at 778 eV and the high intense shoulder at 780 eV. These features are related to the XMCD signal of the Co^{2+} ions. If the contribution of the Co^{2+} ions is included through a weighted sum (red lines) of the

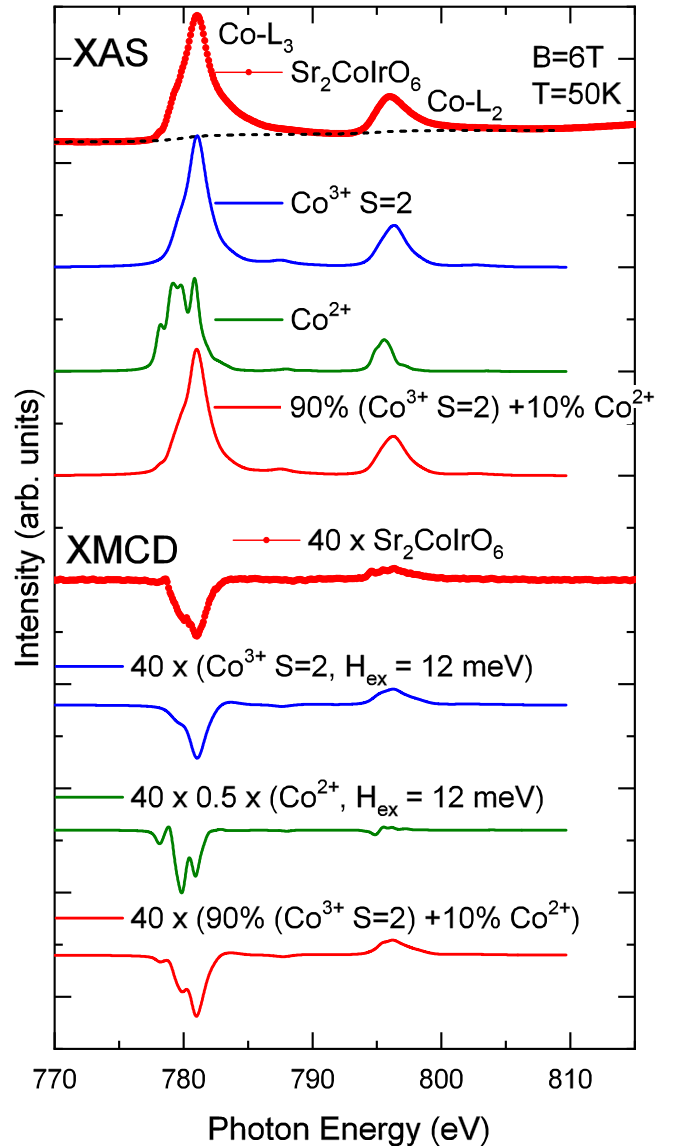


FIG. 3: Experimental Co- $L_{2,3}$ XAS and XMCD spectra of $\text{Sr}_2\text{CoIrO}_6$ (red circles) and theoretical simulations: calculated spectra of $\text{Co}^{3+} S = 2$ (blue lines), Co^{2+} (green lines) and a weighted sum of calculated spectra of $\text{Co}^{3+} S = 2$ and of Co^{2+} (red lines) for $H_{ex} = 12 \text{ meV}$. The simulated XMCD were normalized to the height of the experimental XMCD. The dotted line stands for the edge jump.

calculated XMCD (XAS) spectrum of $\text{Co}^{3+} S = 2$ and that of Co^{2+} (green lines) the agreement with the experimental XMCD (XAS) spectrum of $\text{Sr}_2\text{CoIrO}_6$ becomes excellent all over the energy range. The simulation provides further evidence for the coexistence of a majority (90%) of Co^{3+} ions in the $S = 2$ state and a minority (10%) of Co^{2+} ions in $\text{Sr}_2\text{CoIrO}_6$.

Important to mention is that the size of the measured Co XMCD is about 11 times smaller than the calculated Co XMCD spectrum if the exchange field H_{ex} is assumed to be zero (paramagnetic case). The small size of the experimental Co XMCD signal is due to the fact

the cobalt ions are antiferromagnetically ordered, as revealed by previous neutron diffraction measurements²², and only the canting moment induced by the applied field contributes to the XMCD signal. The size of the experimental XMCD signal was reproduced by using an exchange field of 12 meV, a value that matches nicely with the ordering temperature $T_{N1} = 130$ K of the cobalt moments²³.

The large difference in intensity of the measured dichroic signal between the L_3 and L_2 edges shown in Fig. 3 is a clear signature that the Co ions have a relevant unquenched orbital moment. To be quantitative, we now apply the sum rules for XMCD developed by Thole et al.⁵¹ and Carra et al.⁵², which provide the orbital to spin ratio:

$$\frac{L_z}{2S_z + 7T_z} = \frac{2}{3} \cdot \frac{\int_{L_{2,3}} (\sigma^+ - \sigma^-) dE}{\int_{L_3} (\sigma^+ - \sigma^-) dE - 2 \int_{L_2} (\sigma^+ - \sigma^-) dE} \quad (1)$$

where T_z denotes the intra-atomic magnetic dipole moment. From the experiments we obtain a value of 0.25 for this quantity. Our configuration-interaction full-multiplet simulation with the weighted sum of 90% Co^{3+} and 10% Co^{2+} provides a value of 0.235, which is in very good agreement with the experiment. This is fully consistent with the fact that our simulation reproduces very well the experimental line shapes of the XAS and XMCD spectra as displayed in Fig. 3.

We would like to note that for 3d transition metal ions in an octahedral symmetry this term T_z is a small number⁵³ and is expected to be a little increased by the local distortion existing in the present compound. Our configuration interaction full-multiplet calculations indeed found that the magnetic dipole moment is small compared to the large spin moment the HS Co^{3+} and Co^{2+} : $T_z/S_z = -0.02$. In other words, the above mentioned XMCD sum rule provides in our case directly the important quantum number of orbital to spin ratio, $L_z/2S_z$.

D. Ir- $L_{2,3}$ XMCD

The Ir- $L_{2,3}$ XAS and XMCD spectra of $\text{Sr}_2\text{CoIrO}_6$ are reported as red and blue lines, respectively, in Fig. 4, together with the integral of the XMCD signal (green lines). Very important, the Ir- L_2 and L_3 XMCD signals have almost equal intensity but opposite sign, which results in a very small integrated intensity (green line) over the Ir- $L_{2,3}$ energy range. Kolchinskaya et al.²⁴ reported a similar (but not identical) Ir- $L_{2,3}$ XMCD spectrum for $\text{Sr}_2\text{CoIrO}_6$. A vanishing integrated XMCD intensity indicates that the orbital moment of Ir^{5+} in $\text{Sr}_2\text{CoIrO}_6$ is nearly quenched. The spectral lineshape of the present compound is quite different from that of the Ir- $L_{2,3}$ XMCD spectrum of $\text{Sr}_2\text{Co}_{0.5}\text{Ir}_{0.5}\text{O}_4$, where the measured dichroic signal at the L_3 edge is much larger

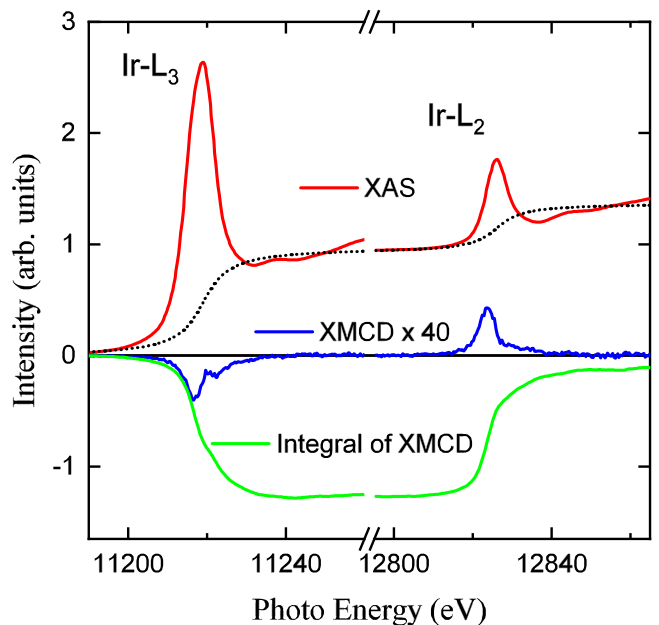


FIG. 4: Experimental Ir- $L_{2,3}$ XAS (red line) and XMCD (blue line) spectra measured on $\text{Sr}_2\text{CoIrO}_6$. The green line is the integration over energy of the XMCD signal and the dotted line stands for the edge jump. The spectra were measured at 2 K with a magnetic field of 17 T and using the TFY mode.

than that at L_2 edge¹⁶. In order to be quantitative we applied the sum rules to our XMCD data and estimated the orbital to spin ratio to be very small and positive: $L_z/(2S_z + 7T_z) = 0.03$. This is an order of magnitude smaller than the $L_z/(2S_z + 7T_z) = 0.45$ value in $\text{Sr}_2\text{Co}_{0.5}\text{Ir}_{0.5}\text{O}_4$ ¹⁶.

V. DISCUSSION

The Ir- $L_{2,3}$ XMCD spectrum of $\text{Sr}_2\text{CoIrO}_6$ is very different from the usual spectrum measured on other Ir^{5+} oxides, like the layered $\text{Sr}_2\text{Co}_{0.5}\text{Ir}_{0.5}\text{O}_4$ ¹⁶ or the double perovskites Sr_2MIrO_6 with $\text{M} = \text{Sc}, \text{In}$ and Fe ²⁵. In fact, the typical Ir^{5+} XMCD spectrum exhibits an Ir- L_2 signal much smaller than the Ir- L_3 signal. The resulting XMCD integral is large and reflects the presence of a significant orbital moment, as also shown by the application of the sum rules giving an $L_z/2S_z$ ratio ranging from 0.26 (in $\text{Sr}_2\text{FeIrO}_6$) to 0.8 (in $\text{Sr}_2\text{InIrO}_6$). In $\text{Sr}_2\text{Co}_{0.5}\text{Ir}_{0.5}\text{O}_4$ ¹⁶ and $\text{Sr}_2\text{ScIrO}_6$ ²⁵ the $L_z/2S_z$ ratio is close to 0.5, i.e. the expected value for a $J_{eff} = 0$ ground state. To our knowledge, $\text{Sr}_2\text{CoIrO}_6$ is the only Ir^{5+} oxide displaying a large Ir- L_2 XMCD signal, with intensity similar to the Ir- L_3 one, and, hence, having $L_z/2S_z$ close to zero. The question that arises now is what physical mechanism is causing the seemingly vanishing of the orbital moment in the present compound. In order to answer to this question and to determine what is the nature of the ground state of Ir^{5+} ions in $\text{Sr}_2\text{CoIrO}_6$ we have per-

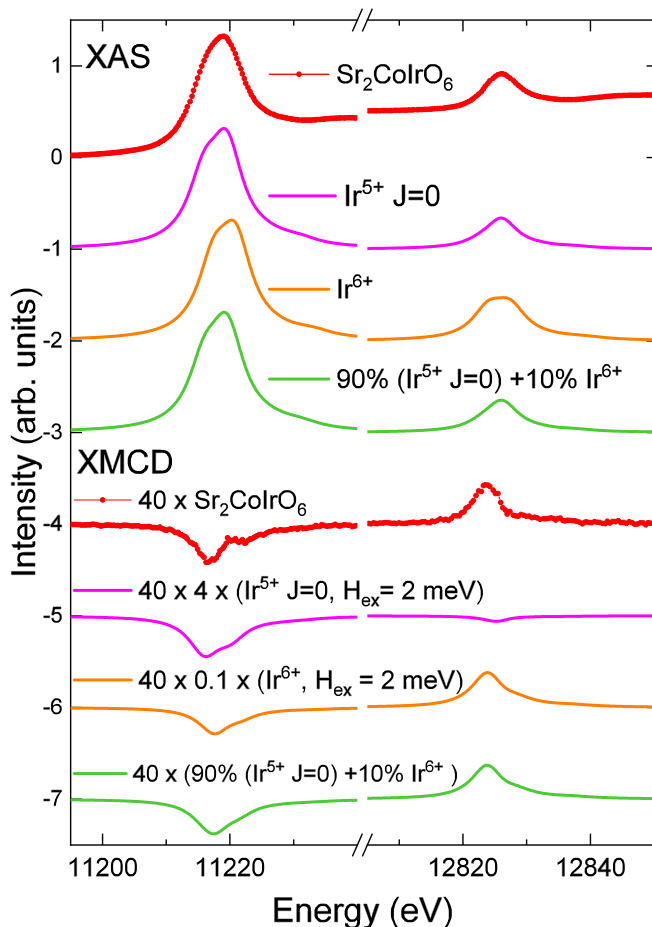


FIG. 5: Experimental Ir- $L_{2,3}$ XAS and XMCD spectra of $\text{Sr}_2\text{CoIrO}_6$ (red circles) and theoretical simulations: calculated spectra of Ir^{5+} $J_{eff} = 0$ (magenta lines), Ir^{6+} (orange lines) and a weighted sum of calculated spectra of Ir^{5+} $J_{eff} = 0$ and of Ir^{6+} (green lines) for $H_{ex} = 2$ meV. The simulated XMCD were normalized to the height of the experimental XMCD.

formed configuration-interaction cluster calculations for the Ir- $L_{2,3}$ XAS and XMCD spectra.

Considering the fact that we have found about 10% Co^{2+} ions in this formally Co^{3+} system, we investigate the possibility that the measured XMCD signal contains contributions from the presence of Ir^{4+} and/or Ir^{6+} ions in this otherwise Ir^{5+} material. Starting with the Ir^{4+} scenario, we note that the XMCD spectrum of Ir^{4+} oxides is well known to exhibit a very small Ir- L_2 XMCD signal^{25,54,55}. Since this cannot generate the large Ir- L_2 XMCD signal observed in our $\text{Sr}_2\text{CoIrO}_6$, we can safely rule out the possibility that the XMCD of $\text{Sr}_2\text{CoIrO}_6$ is produced by Ir^{4+} ions. Considering now the Ir^{6+} scenario, we would like to remark that Ir^{6+} ions have a d^3 configuration with the spins of three electrons in the t_{2g} shell all parallel to form a $S = 3/2$ spin state. In this situation of half-filled t_{2g} shell the orbital moment is naturally zero or close to. As a consequence, the XMCD spectrum of Ir^{6+} oxides has the L_3 and L_2 signals similar

in size. This is then a promising scenario to follow.

In Fig. 5, we have plotted the experimental XAS and XMCD spectra together with the simulations for the Ir^{5+} $J_{eff} = 0$ (magenta lines) and Ir^{6+} $S = 3/2$ (orange lines). The parameters for the simulations are listed in Ref.³⁴. We can clearly observe that the calculated XMCD signal at the L_2 is small for the Ir^{5+} and that it is large for the Ir^{6+} , confirming our considerations described in the above paragraph. We now compose a weighted sum of the Ir^{5+} and Ir^{6+} simulations, and the result for a 90:10 ratio is also displayed in Fig. 5 (green lines). This weighted sum can nicely reproduce the line shape of both the experimental XAS and XMCD spectra of $\text{Sr}_2\text{CoIrO}_6$. Hence, the anomalous spectral shape of the Ir- $L_{2,3}$ XMCD of $\text{Sr}_2\text{CoIrO}_6$ can be explained by the presence of 10% magnetic Ir^{6+} ions in a matrix of Van Vleck paramagnetic Ir^{5+} ions. Our finding is not inconsistent with a previous diffraction study, where the bond valence sums predicted in $\text{Sr}_2\text{CoIrO}_6$ a partial amount of iridium ions to be in the 6+ valence state²².

In our full multiplet atomic calculations the orbital moment of Ir^{5+} ions is quite large, with an isotropic ratio of $L_z/2S_z = 0.50$ ($L_z/(2S_z + 7T_z) = 0.59$). This is the orbital-to-spin moment ratio expected for the $J_{eff} = 0$ ground state¹⁶. The calculated orbital moment of the Ir^{6+} ions is very small, as expected for the $S = 3/2$ state: $L_z/2S_z = -0.05$ ($L_z/(2S_z + 7T_z) = -0.05$). The application of the sum rules to our configuration-interaction full-multiplet simulation of the Ir- $L_{2,3}$ XMCD with the weighted sum of 90% Ir^{5+} and 10% Ir^{6+} provides a value of 0.026, which is in excellent agreement with the experiment.

It is interesting that a 90:10 weighted sum simulation reproduce the experimental spectra quite accurately. The amount of 10% Ir^{6+} corresponds very well with the presence of 10% Co^{2+} as we have found earlier. It seems that the two quantities compensate each other, i.e. that the charge balance requirement is fulfilled here. This in turn suggests also that our material is stoichiometric and that there is a competition between the $\text{Ir}^{5+}\text{-Co}^{3+}$ and the $\text{Ir}^{6+}\text{-Co}^{2+}$ configurations in this double perovskite.

It is important to note that the calculated XMCD of the majority Van Vleck Ir^{5+} ions in an applied field of 17 Tesla is roughly half of the size of the needed contribution in the weighted sum to simulate the experimental XMCD spectrum. Such a difference in size can be explained by the presence of a small exchange field of 2 meV acting on the paramagnetic Van Vleck Ir^{5+} ions. The exchange field would be generated by the canting of the antiferromagnetic ordered Co moments, which is induced by the 17 T applied magnetic field, or by the Ir^{6+} ions. A similar exchange field of 2 meV was also used for the calculation of the XMCD of the Ir^{6+} ions. Differently from the paramagnetic Van Vleck Ir^{5+} ions, in our model the Ir^{6+} ions are antiferromagnetically ordered because paramagnetic Ir^{6+} ions would produce a Curie-like divergent susceptibility, which is not observed in the magnetic susceptibility of $\text{Sr}_2\text{CoIrO}_6$ as displayed

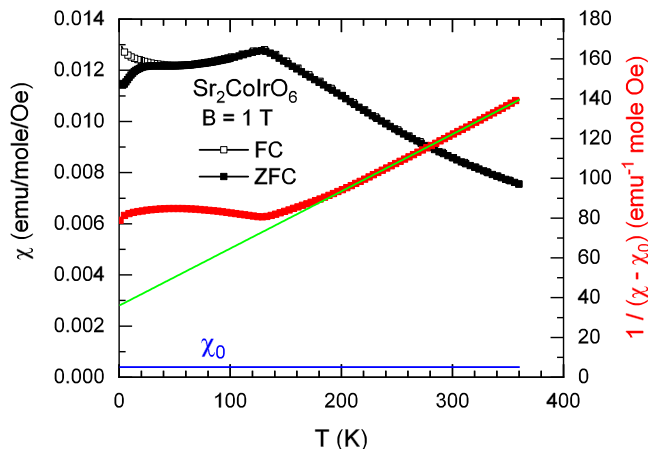


FIG. 6: Temperature dependence of the molar and inverse molar magnetic susceptibilities of $\text{Sr}_2\text{CoIrO}_6$ at fields of 1 T in the temperature range of 2-380 K. The Curie-Weiss fit of the inverse susceptibility is shown as green line.

in Fig. 6. Instead the magnetic susceptibility exhibits a maximum at around 20 K, indicative for the ordering temperature T_{N2} of the Ir^{6+} sublattice.

As final check of our $\text{Ir}^{6+}/\text{Ir}^{5+}$ two-component scenario for the magnetism of the iridium ions in $\text{Sr}_2\text{CoIrO}_6$, we performed a Curie-Weiss analysis of the magnetic susceptibility. The T-dependent molar magnetic inverse susceptibility $1/(\chi - \chi_0)_{mol}$ (red points) of $\text{Sr}_2\text{CoIrO}_6$ is displayed in Fig. 6. The good linearity of $1/(\chi - \chi_0)_{mol}$ vs. T indicates Curie-Weiss behavior at temperatures above 200 K. Here, we have used $\chi_{0,mol} = 4 \times 10^{-4} \text{ emu mol}^{-1} \text{ Oe}^{-1}$ as also indicated in Fig. 6 (blue line). From the Curie-Weiss fit (green line) we extracted an effective magnetic moment μ_{eff} of $5.3 \mu_B$ and a Weiss-constant θ_W of $\sim 125 \text{ K}$. The $|\theta_W|/T_{N1}$ ratio very close to 1 suggests that frustration of the exchange interactions is readily lifted in this compound, like in SrLaNiIrO_6 where $|\theta_W|/T_{N1}$ ratio is ~ 1.2 . A very different situation is observed in Ba_2BOsO_6 (B = Sc, Y, In) and SrLaCuIrO_6 , where $|\theta_W|/T_{N1}$ ratios of $\sim 6-8$ indicate the presence of a large degree of frustration^{56,57}.

From our full atomic multiplet calculations we found a Van Vleck paramagnetic contribution of $\chi_{0,mol} = 8.2 \times 10^{-4} \text{ emu mol}^{-1} \text{ Oe}^{-1}$ for the $J_{eff} = 0 \text{ Ir}^{5+}$ ions. This is larger than the experimentally extracted value of $\chi_{0,mol} = 4 \times 10^{-4} \text{ emu mol}^{-1} \text{ Oe}^{-1}$. From the sum of the diamagnetic susceptibilities, obtained from standard charts⁵⁸, of the individual ions in the compound we estimate that the temperature independent diamagnetic contribution amounts to about $-1.4 \times 10^{-4} \text{ emu mol}^{-1} \text{ Oe}^{-1}$. Although we may not be able to fully explain the discrepancy between the calculated and experimental values, it is fair to state that the agreement is quite

satisfactory, i.e. 8.2×10^{-4} vs. 5.4×10^{-4} ($= 4 \times 10^{-4} + 1.4 \times 10^{-4}$) $\text{emu mol}^{-1} \text{ Oe}^{-1}$. A variety of values in the same range were reported for $\chi_{0,mol}$ of other Ir^{5+} double perovskites: from 10×10^{-4} and $8.7 \times 10^{-4} \text{ emu mol}^{-1} \text{ Oe}^{-1}$ in SrLaCuIrO_6 ⁵⁷ and Sr_2YIrO_6 ¹⁵, respectively, to relatively smaller numbers (5.8×10^{-4} , 5×10^{-4} , 3.5×10^{-4} and $3.9 \times 10^{-4} \text{ emu mol}^{-1} \text{ Oe}^{-1}$) in Ba_2YIrO_6 ¹⁹, SrLaNiIrO_6 , SrLaMgIrO_6 and SrLaZnIrO_6 ⁵⁹. The total effective magnetic moment of $\text{Sr}_2\text{CoIrO}_6$ as given by our cluster calculations^{33,34} in the hypothesis of cobalt site 90% occupied by Co^{3+} and 10% by Co^{2+} , and iridium site 10% occupied by Ir^{6+} , is $\mu_{eff}(total) = \sqrt{0.9 \times 4.96^2 + 0.1 \times 5.43^2 + 0.1 \times 3.07^2} = 5.1 \mu_B$. This value is in good agreement with the value μ_{eff} of $5.3 \mu_B$ extracted from the Curie-Weiss fit. If on the other hand a pure Ir^{5+} scenario is considered the calculated total μ_{eff} is reduced to $5.0 \mu_B$. On the base of the above analysis, we can conclude that within the limits of the sensitivity of the magnetic susceptibility the two-component scenario provides a good agreement with the experimental data.

VI. SUMMARY

To summarize, XAS and XMCD measurements at the Co- $L_{2,3}$ edge demonstrate a Co^{3+} HS state in the double perovskite $\text{Sr}_2\text{CoIrO}_6$. This state is not pure, as our XAS and XMCD also reveal the presence of 10% cobalt ions in the Co^{2+} state. Our Ir- $L_{2,3}$ edge XAS shows that iridium has mainly the 5+ valence. However, by a comparison of the experimental Ir- $L_{2,3}$ XMCD data with full atomic multiplet calculations we were able to clarify that the signal at the L_2 edge is mainly due to a contribution from Ir^{6+} ions. Hence, the unusual shape of the XMCD spectrum of $\text{Sr}_2\text{CoIrO}_6$ can be explained with the presence of 10% of $S = 3/2 \text{ Ir}^{6+}$ ions coexisting with 90% $J_{eff} = 0 \text{ Ir}^{5+}$ ions. The presence of equal amounts of ions with a different valence state in $\text{Sr}_2\text{CoIrO}_6$ is probably driven by the delicate balance between the chemical stability for a $\text{Ir}^{5+}\text{-Co}^{3+}$ configuration versus that for a $\text{Ir}^{6+}\text{-Co}^{2+}$ configuration.

Acknowledgments

K. C. benefited from support of the Deutsche Forschungsgemeinschaft (DFG) via the Project SE 1441/1-2. The research in Dresden was partially supported by the DFG through SFB 1143 (project-id 247310070) and by the Max Planck-POSTECH-Hsinchu Center for Complex Phase Materials. We gratefully acknowledge SOLEIL, HASYLAB, ESRF and NSRRC for providing us with synchrotron beamtime.

* Electronic address: stefano.agrestini@cells.es

¹ B. J. Kim, H. Jin, S. J. Moon, J.-Y. Kim, B.-G. Park, C. S.

- Leem, J. Yu, T. W. Noh, C. Kim, S.-J. Oh, et al., Phys. Rev. Lett. **101**, 076402 (2008), URL <https://link.aps.org/doi/10.1103/PhysRevLett.101.076402>.
- ² B. J. Kim, H. Ohsumi, T. Komesu, S. Sakai, T. Morita, H. Takagi, and T. Arima, Science **323**, 1329 (2009), ISSN 0036-8075, <https://science.sciencemag.org/content/323/5919/1329.full.pdf>, URL <https://science.sciencemag.org/content/323/5919/1329>.
- ³ G. Jackeli and G. Khaliullin, Phys. Rev. Lett. **102**, 017205 (2009), URL <https://link.aps.org/doi/10.1103/PhysRevLett.102.017205>.
- ⁴ J. c. v. Chaloupka, G. Jackeli, and G. Khaliullin, Phys. Rev. Lett. **105**, 027204 (2010), URL <https://link.aps.org/doi/10.1103/PhysRevLett.105.027204>.
- ⁵ K. W. Plumb, J. P. Clancy, L. J. Sandilands, V. V. Shankar, Y. F. Hu, K. S. Burch, H.-Y. Kee, and Y.-J. Kim, Phys. Rev. B **90**, 041112(R) (2014), URL <https://link.aps.org/doi/10.1103/PhysRevB.90.041112>.
- ⁶ S. Agrestini, C.-Y. Kuo, K.-T. Ko, Z. Hu, D. Kasinathan, H. B. Vasili, J. Herrero-Martin, S. M. Valvidares, E. Pellegrin, L.-Y. Jang, et al., Phys. Rev. B **96**, 161107(R) (2017), URL <https://link.aps.org/doi/10.1103/PhysRevB.96.161107>.
- ⁷ A. Kitaev, Annals of Physics **321**, 2 (2006), ISSN 0003-4916, January Special Issue, URL <http://www.sciencedirect.com/science/article/pii/S0003491605002381>.
- ⁸ S. Nakatsuji, S.-i. Ikeda, and Y. Maeno, Journal of the Physical Society of Japan **66**, 1868 (1997), URL <https://doi.org/10.1143/JPSJ.66.1868>.
- ⁹ M. Braden, G. André, S. Nakatsuji, and Y. Maeno, Phys. Rev. B **58**, 847 (1998), URL <https://link.aps.org/doi/10.1103/PhysRevB.58.847>.
- ¹⁰ G. Khaliullin, Phys. Rev. Lett. **111**, 197201 (2013), URL <https://link.aps.org/doi/10.1103/PhysRevLett.111.197201>.
- ¹¹ O. N. Meetei, W. S. Cole, M. Randeria, and N. Trivedi, Phys. Rev. B **91**, 054412 (2015), URL <https://link.aps.org/doi/10.1103/PhysRevB.91.054412>.
- ¹² J. c. v. Chaloupka and G. Khaliullin, Phys. Rev. Lett. **116**, 017203 (2016), URL <https://link.aps.org/doi/10.1103/PhysRevLett.116.017203>.
- ¹³ K. Pajskr, P. Novák, V. Pokorný, J. Kolorenč, R. Arita, and J. Kuneš, Phys. Rev. B **93**, 035129 (2016), URL <https://link.aps.org/doi/10.1103/PhysRevB.93.035129>.
- ¹⁴ C. Svoboda, M. Randeria, and N. Trivedi, Phys. Rev. B **95**, 014409 (2017), URL <https://link.aps.org/doi/10.1103/PhysRevB.95.014409>.
- ¹⁵ G. Cao, T. F. Qi, L. Li, J. Terzic, S. J. Yuan, L. E. DeLong, G. Murthy, and R. K. Kaul, Phys. Rev. Lett. **112**, 056402 (2014), URL <https://link.aps.org/doi/10.1103/PhysRevLett.112.056402>.
- ¹⁶ S. Agrestini, C.-Y. Kuo, K. Chen, Y. Utsumi, D. Mikhailova, A. Rogalev, F. Wilhelm, T. Förster, A. Matsumoto, T. Takayama, et al., Phys. Rev. B **97**, 214436 (2018), URL <https://link.aps.org/doi/10.1103/PhysRevB.97.214436>.
- ¹⁷ M. Kusch, V. M. Katukuri, N. A. Bogdanov, B. Büchner, T. Dey, D. V. Efremov, J. E. Hamann-Borrero, B. H. Kim, M. Krisch, A. Maljuk, et al., Phys. Rev. B **97**, 064421 (2018), URL <https://link.aps.org/doi/10.1103/PhysRevB.97.064421>.
- ¹⁸ S. Bhowal, S. Baidya, I. Dasgupta, and T. Saha-Dasgupta, Phys. Rev. B **92**, 121113(R) (2015), URL <https://link.aps.org/doi/10.1103/PhysRevB.92.121113>.
- ¹⁹ T. Dey, A. Maljuk, D. V. Efremov, O. Kataeva, S. Gass, C. G. F. Blum, F. Steckel, D. Gruner, T. Ritschel, A. U. B. Wolter, et al., Phys. Rev. B **93**, 014434 (2016), URL <https://link.aps.org/doi/10.1103/PhysRevB.93.014434>.
- ²⁰ L. T. Corredor, G. Aslan-Cansever, M. Sturza, K. Manna, A. Maljuk, S. Gass, T. Dey, A. U. B. Wolter, O. Kataeva, A. Zimmermann, et al., Phys. Rev. B **95**, 064418 (2017), URL <https://link.aps.org/doi/10.1103/PhysRevB.95.064418>.
- ²¹ J. Terzic, H. Zheng, F. Ye, H. D. Zhao, P. Schlottmann, L. E. De Long, S. J. Yuan, and G. Cao, Phys. Rev. B **96**, 064436 (2017), URL <https://link.aps.org/doi/10.1103/PhysRevB.96.064436>.
- ²² N. Narayanan, D. Mikhailova, A. Senyshyn, D. M. Trots, R. Laskowski, P. Blaha, K. Schwarz, H. Fuess, and H. Ehrenberg, Phys. Rev. B **82**, 024403 (2010), URL <https://link.aps.org/doi/10.1103/PhysRevB.82.024403>.
- ²³ D. Mikhailova, N. Narayanan, W. Gruner, A. Voss, A. Senyshyn, D. M. Trots, H. Fuess, and H. Ehrenberg, Inorganic Chemistry **49**, 10348 (2010), PMID: 20964307, URL <https://doi.org/10.1021/ic100973p>.
- ²⁴ A. Kolchinskaya, P. Komissinskiy, M. B. Yazdi, M. Vafae, D. Mikhailova, N. Narayanan, H. Ehrenberg, F. Wilhelm, A. Rogalev, and L. Alff, Phys. Rev. B **85**, 224422 (2012), URL <https://link.aps.org/doi/10.1103/PhysRevB.85.224422>.
- ²⁵ M. A. Laguna-Marco, P. Kayser, J. A. Alonso, M. J. Martínez-Lope, M. van Veenendaal, Y. Choi, and D. Haskel, Phys. Rev. B **91**, 214433 (2015), URL <https://link.aps.org/doi/10.1103/PhysRevB.91.214433>.
- ²⁶ P. Ohresser, E. Otero, F. Choueikani, K. Chen, S. Stanescu, F. Deschamps, T. Moreno, F. Polack, B. Lagarde, J.-P. Daguere, et al., Review of Scientific Instruments **85**, 013106 (2014), URL <https://doi.org/10.1063/1.4861191>.
- ²⁷ A. Rogalev and F. Wilhelm, The Physics of Metals and Metallography **116**, 1285 (2015), ISSN 1555-6190, URL <https://doi.org/10.1134/S0031918X15130013>.
- ²⁸ B. Henke, E. Gullikson, and J. Davis, Atomic Data and Nuclear Data Tables **54**, 181 (1993), ISSN 0092-640X, URL <http://www.sciencedirect.com/science/article/pii/S0092640X83710132>.
- ²⁹ M. W. Haverkort, M. Zwierzycki, and O. K. Andersen, Phys. Rev. B **85**, 165113 (2012), URL <https://link.aps.org/doi/10.1103/PhysRevB.85.165113>.
- ³⁰ Y. Lu, M. Höppner, O. Gunnarsson, and M. W. Haverkort, Phys. Rev. B **90**, 085102 (2014), URL <https://link.aps.org/doi/10.1103/PhysRevB.90.085102>.
- ³¹ M. W. Haverkort, G. Sangiovanni, P. Hansmann, A. Toschi, Y. Lu, and S. Macke, EPL (Europhysics Letters) **108**, 57004 (2014), URL <http://stacks.iop.org/0295-5075/108/i=5/a=57004>.
- ³² K. Koepernik and H. Eschrig, Phys. Rev. B **59**, 1743 (1999), URL <https://link.aps.org/doi/10.1103/PhysRevB.59.1743>.
- ³³ CoO₆ cluster parameters [eV]: $U_{dd} = 5.5$, $U_{pd} = 7.0$, ionic crystal field $10D_q = 0.545$, $\Delta t_{2g} = -0.265$, $\Delta e_g = -0.047$, charge transfer energy $\Delta_{CT} = 2.0$, hybridization $V(x^2 - y^2) = 2.52$, $V(z^2) = 2.63$, $V(xy) = 1.38$, $V(xz) = V(yz) =$

- 1.43, ligand-crystal field $10Dq^{lig} = 1.0$, spin-orbit coupling $\zeta_{3d} = 0.074$, exchange field $H_{ex} = 0.012$ and magnetic field 6 T. The Slater integrals were reduced to 80% of Hartree-Fock values. In the calculations of the effective moment at high temperature the exchange field was considered to be zero.
- ³⁴ IrO6 cluster parameters [eV]: $U_{dd} = 1.0$, $U_{pd} = 2.0$, ionic crystal field $10Dq = 2.3$, $\Delta t_{2g} = 0.1$, $\Delta e_g = 0.125$, charge transfer energy $\Delta_{CT} = -1.5$, hybridization $V(x^2 - y^2) = 5.21$, $V(z^2) = 5.08$, $V(xy) = 2.835$, $V(xz) = V(yz) = 2.915$, ligand-crystal field $10Dq^{lig} = 0.93$, spin-orbit coupling $\zeta_{5d} = 0.4$, exchange field $H_{ex} = 0.002$ and magnetic field 17 T. The Slater integrals were reduced to 70% of Hartree-Fock values. In the calculations of the effective moment at high temperature the exchange field was considered to be zero.
- ³⁵ J. Wong, F. W. Lytle, R. P. Messmer, and D. H. Maylotte, *Phys. Rev. B* **30**, 5596 (1984), URL <https://link.aps.org/doi/10.1103/PhysRevB.30.5596>.
- ³⁶ C. T. Chen and F. Sette, *Physica Scripta* **1990**, 119 (1990), URL <http://stacks.iop.org/1402-4896/1990/i=T31/a=016>.
- ³⁷ C. Mitra, Z. Hu, P. Raychaudhuri, S. Wirth, S. I. Csiszar, H. H. Hsieh, H.-J. Lin, C. T. Chen, and L. H. Tjeng, *Phys. Rev. B* **67**, 092404 (2003), URL <https://link.aps.org/doi/10.1103/PhysRevB.67.092404>.
- ³⁸ T. Burnus, Z. Hu, M. W. Haverkort, J. C. Cezar, D. Flahaut, V. Hardy, A. Maignan, N. B. Brookes, A. Tanaka, H. H. Hsieh, et al., *Phys. Rev. B* **74**, 245111 (2006), URL <https://link.aps.org/doi/10.1103/PhysRevB.74.245111>.
- ³⁹ T. Burnus, Z. Hu, H. H. Hsieh, V. L. J. Joly, P. A. Joy, M. W. Haverkort, H. Wu, A. Tanaka, H.-J. Lin, C. T. Chen, et al., *Phys. Rev. B* **77**, 125124 (2008), URL <https://link.aps.org/doi/10.1103/PhysRevB.77.125124>.
- ⁴⁰ K. Baroudi, C. Yim, H. Wu, Q. Huang, J. H. Roudebush, E. Vavilova, H.-J. Grafe, V. Kataev, B. Buechner, H. Ji, et al., *Journal of Solid State Chemistry* **210**, 195 (2014), ISSN 0022-4596, URL <http://www.sciencedirect.com/science/article/pii/S002245961300563X>.
- ⁴¹ J.-H. Choy, D.-K. Kim, S.-H. Hwang, G. Demazeau, and D.-Y. Jung, *Journal of the American Chemical Society* **117**, 8557 (1995), URL <https://doi.org/10.1021/ja00138a010>.
- ⁴² S. Mugavero III, M. Smith, W.-S. Yoon, and H.-C. zurLoye, *Angewandte Chemie International Edition* **48**, 215 (2009), URL <https://onlinelibrary.wiley.com/doi/abs/10.1002/anie.200804045>.
- ⁴³ J.-M. Chen, Y.-Y. Chin, M. Valldor, Z. Hu, J.-M. Lee, S.-C. Haw, N. Hiraoka, H. Ishii, C.-W. Pao, K.-D. Tsuei, et al., *Journal of the American Chemical Society* **136**, 1514 (2014), PMID: 24410074, URL <https://doi.org/10.1021/ja4114006>.
- ⁴⁴ S. Esser, C. F. Chang, C.-Y. Kuo, S. Merten, V. Roddatis, T. D. Ha, A. Jesche, V. Moshnyaga, H.-J. Lin, A. Tanaka, et al., *Phys. Rev. B* **97**, 205121 (2018), URL <https://link.aps.org/doi/10.1103/PhysRevB.97.205121>.
- ⁴⁵ Z. Hu, H. Wu, M. W. Haverkort, H. H. Hsieh, H. J. Lin, T. Lorenz, J. Baier, A. Reichl, I. Bonn, C. Felser, et al., *Phys. Rev. Lett.* **92**, 207402 (2004), URL <https://link.aps.org/doi/10.1103/PhysRevLett.92.207402>.
- ⁴⁶ M. W. Haverkort, Z. Hu, J. C. Cezar, T. Burnus, H. Hartmann, M. Reuther, C. Zobel, T. Lorenz, A. Tanaka, N. B. Brookes, et al., *Phys. Rev. Lett.* **97**, 176405 (2006), URL <https://link.aps.org/doi/10.1103/PhysRevLett.97.176405>.
- ⁴⁷ C. F. Chang, Z. Hu, H. Wu, T. Burnus, N. Hollmann, M. Benomar, T. Lorenz, A. Tanaka, H.-J. Lin, H. H. Hsieh, et al., *Phys. Rev. Lett.* **102**, 116401 (2009), URL <https://link.aps.org/doi/10.1103/PhysRevLett.102.116401>.
- ⁴⁸ T. Burnus, Z. Hu, H. Wu, J. C. Cezar, S. Niitaka, H. Takagi, C. F. Chang, N. B. Brookes, H.-J. Lin, L. Y. Jang, et al., *Phys. Rev. B* **77**, 205111 (2008), URL <https://link.aps.org/doi/10.1103/PhysRevB.77.205111>.
- ⁴⁹ T. Burnus, Z. Hu, H. Wu, J. C. Cezar, S. Niitaka, H. Takagi, C. F. Chang, N. B. Brookes, H.-J. Lin, L. Y. Jang, et al., *Phys. Rev. B* **77**, 205111 (2008), URL <https://link.aps.org/doi/10.1103/PhysRevB.77.205111>.
- ⁵⁰ N. Hollmann, Z. Hu, M. Valldor, A. Maignan, A. Tanaka, H. H. Hsieh, H.-J. Lin, C. T. Chen, and L. H. Tjeng, *Phys. Rev. B* **80**, 085111 (2009), URL <https://link.aps.org/doi/10.1103/PhysRevB.80.085111>.
- ⁵¹ B. T. Thole, P. Carra, F. Sette, and G. van der Laan, *Phys. Rev. Lett.* **68**, 1943 (1992), URL <https://link.aps.org/doi/10.1103/PhysRevLett.68.1943>.
- ⁵² P. Carra, B. T. Thole, M. Altarelli, and X. Wang, *Phys. Rev. Lett.* **70**, 694 (1993), URL <https://link.aps.org/doi/10.1103/PhysRevLett.70.694>.
- ⁵³ Y. Teramura, A. Tanaka, and T. Jo, *Journal of the Physical Society of Japan* **65**, 1053 (1996), URL <https://doi.org/10.1143/JPSJ.65.1053>.
- ⁵⁴ M. A. Laguna-Marco, D. Haskel, N. Souza-Neto, J. C. Lang, V. V. Krishnamurthy, S. Chikara, G. Cao, and M. van Veenendaal, *Phys. Rev. Lett.* **105**, 216407 (2010), URL <https://link.aps.org/doi/10.1103/PhysRevLett.105.216407>.
- ⁵⁵ D. Haskel, G. Fabbris, M. Zhernenkov, P. P. Kong, C. Q. Jin, G. Cao, and M. van Veenendaal, *Phys. Rev. Lett.* **109**, 027204 (2012), URL <https://link.aps.org/doi/10.1103/PhysRevLett.109.027204>.
- ⁵⁶ H. L. Feng, K. Yamaura, L. H. Tjeng, and M. Jansen, *Journal of Solid State Chemistry* **243**, 119 (2016), ISSN 0022-4596, URL <http://www.sciencedirect.com/science/article/pii/S0022459616303310>.
- ⁵⁷ K. K. Wolff, L. H. Tjeng, and M. Jansen, *Solid State Communications* **289**, 43 (2019), ISSN 0038-1098, URL <http://www.sciencedirect.com/science/article/pii/S0038109818306616>.
- ⁵⁸ G. A. Bain and J. F. Berry, *Journal of Chemical Education* **85**, 532 (2008), URL <https://doi.org/10.1021/ed085p532>.
- ⁵⁹ K. K. Wolff, S. Agrestini, A. Tanaka, M. Jansen, and L. H. Tjeng, *Zeitschrift für anorganische und allgemeine Chemie* **643**, 2095 (2017), URL <https://onlinelibrary.wiley.com/doi/abs/10.1002/zaac.201700386>.